

## RESEARCH PAPER

# Comparison of Specific Wear Rates of Austenitic and Super Austenitic Stainless Steels at High Temperatures

Dler A. Ahmed<sup>1</sup>, Mohammedtaher M. Mulapeer<sup>2</sup>

<sup>1&2</sup>Department of Mechanical & Mechatronics, College of Engineering, Salahaddin University -Erbil, Iraq

### ABSTRACT:

Due to the relatively high wear rate of the austenitic stainless steel S30400 and the high mechanical properties of the super austenitic stainless steel S31254, it was possible to compare the wear behavior of the two alloys and select the best alloy to extend the service life of sliding parts. In this work, wear tests were performed at five different temperatures (30°C, 140°, 300°C, 460°C, and 570°C) at constant sliding speed, applied load, and sliding distance for both alloys. The specific wear rate of S31254 was more than 50% lower compared to S30400 at the different temperatures, except at 570°C, where it was only 16%. According to scanning electron microscopy and X-ray diffraction, oxide formation on the worn surfaces started at 300°C and increased with increasing temperature. The oxide layers protected the surface and reduced wear and material removal. Overall, S31254 exhibited better wear resistance at various temperatures.

KEY WORDS: S30400, S31254, Specific wear rate, High temperature, Scanning electron microscopy, X-ray diffraction, Oxide phase

DOI: <http://dx.doi.org/10.21271/ZJPAS.34.5.3>

ZJPAS (2022) , 34(5);20-33 .

### 1.INTRODUCTION :

Although austenitic stainless steels (ASS) are broadly used in industries because they have excellent corrosion resistance, their low yield strength restricts applications in harsh environments and may necessitate searching for a suitable substitute (Avilaa *et al.*, 2020), (Alabdullah, Polishetty and Littlefair, 2016), (Moharana *et al.*, 2016). Super austenitic stainless steels (SASS) have superior mechanical properties and corrosion resistance (Polishetty, Alabdullah and Littlefair, 2017), (Qiao *et al.*, 2019). Therefore, SASS has been used in important applications like petrochemical equipment, saltwater pumps, and deep-water oil exploration fittings (Sathiya, Mishra and Shanmugarajan, 2012), (Alabdullah *et al.*, 2017). As a result, it is critical to compare the wear behavior of both alloys under different conditions to determine which is superior in a given application.

Wear behavior is one of the important surface properties for selecting materials that are susceptible to friction and wear (Rababa and Al-Mahasne, 2011), (Suthar *et al.*, 2015). Because wear reduces the service life of components and directly affects the economy. For example, wear is a major problem in mineral processing industries, which occurs in tools and machine parts (Li *et al.*, 2019), (Monga, Gumber and Grover, 2018). A great deal of work has been done on the mechanical properties and surface quality of ASS. Wear behavior has also recently attracted the interest of researchers, however, most of them have studied the wear at room temperature, while in various applications such as engines, refineries, and the food industry, wear occurs at high temperatures (Alvi, Saeidi and Akhtar, 2020), (Ge *et al.*, 2019). Chawla and Saini (Chawla *et al.*, 2013) investigated the effect of machining variables on the wear phenomena of S30400 austenitic stainless steel. They demonstrated that the wear rate increased slightly with load, and

---

#### \* Corresponding Author:

Dler A. Ahmed

E-mail: [dler.ahmad@epu.edu.iq](mailto:dler.ahmad@epu.edu.iq)

#### Article History:

Received: 11/03/2022

Accepted: 29/05/2022

Published: 20/10 /2022

significantly with sliding speed and sliding time due to friction and generated heat. Bahshwan (Bahshwan *et al.*, 2020) investigated the influence of strain hardening on the microstructure and wear rate of austenitic stainless steels. They observed that with increasing strain hardening, the crystal orientation changed and the wear rate decreased, and the hardness increased. Singh and his colleagues (Singh, Sharma and Singh, 2019) improved the wear resistance of austenitic stainless steel by oxide heat treatment. They indicated that a hard oxide layer formed on the surface and protected the surface from wear. Zhang and his colleagues (Zhang, Yin and Yan, 2016) investigated the wear behavior of S31254 at room temperature and in a corrosive environment. They concluded that it has high wear resistance but degraded with the presence of corrosive materials such as seawater, which accelerated the material removal.

There are some works were done on the wear rate at high temperatures for specific materials. For example, Parthasarathi and Borah (Parthasarathi, Borah and Albert, 2013) observed that the coefficient of friction and surface roughness of austenitic stainless steel increased with the increase of temperature from room temperature to 550°C. Also, they indicated that the valley's depth and the width of the wear tracks increased with increasing temperature. Bayata and Alpas (Bayata and Alpas, 2021) investigated the wear behavior of NCF-3015 and Inconel-751 super alloys at high temperatures. They found that the wear increased from room temperature to 350°C and then decreased significantly up to 650°C, due to the formation of different types of oxides. Parthasarathi (Parthasarathi and Duraiselvam, 2010) studied the wear rate of austenitic stainless steel at high temperatures and claimed that the oxide layer began to form at 350°C and more, which protected the surface from the wear. Kennedy (Kennedy, Lu and Baker, 2015) studied the temperature of contact surfaces and proved that the temperature arises in sliding contact surfaces and is the summation of the ambient temperature, the temperature rise due to friction,

and the flash temperature that occurs at the localized contact points.

Based on previous literature, the wear investigation of ASS at room temperature has been adequately conducted. While very few studies were done about the wear rate of SASS. In addition, there is a research gap in the inspection of wear rate in high-temperature conditions for both alloys and comparison between them. The novelty of this work is the investigation of wear rate at high temperatures of both austenitic and super austenitic stainless steel AISI 304 and S31254. The goal of this research is to predict the actual wear behavior which occurs in engines and refineries at high temperatures until 570°C. The temperature range was chosen based on the range of previous literature, e.g.: (Alvi, Saeidi and Akhtar, 2020) worked from RT to 600°C, (Hernandez *et al.*, 2014) from 20°C to 400°C, (Parthasarathi, Borah and Albert, 2013) from RT to 550°C, and (Bayata and Alpas, 2021) from 25°C to 650°C. Scanning electron microscopy (SEM) was used to illustrate the morphology of the worn surfaces, and Xpert high score software was used to measure and interpret the unique diffractions obtained from the X-ray diffraction (XRD) tests.

## 2. Experimental Procedure:

All alloys used in this work were purchased from China from Shandong WanHui Stainless Steel Co. Ltd. The chemical composition of the pins and discs was determined using a metal analyzer model Spectromaxx Spectro Company as shown in Table 1. In addition, the mechanical properties such as the ultimate strength of the alloys were tested using the Universal Testing Machine model TERCO MT 3037, with a specimen diameter of 6 mm and a gauge length of 24 mm according to the ASTM E8 tensile testing standard (ASTM E8, 2010). Furthermore, Vickers hardness was measured using AKASHI testing machine model AVK with a load of 30 kg. f and time of 15 seconds under ASTM E92-17 (ASTM Standard E92-82, 1997), as listed in Table 2. In addition, wear tests were done. Finally, SEM images and XRD technic of the worn surfaces were done.

Table 1: chemical composition of stainless steel alloys AISI 304, S31254, and AISI 2507.

UNS	C	Mn	P	S	Si	Cr	Ni	Mo	Cu	Co
S30400	0.074	1.51	0.0364	0.0072	0.387	17.23	9.79	0.313	0.481	0.293
S31254	0.071	1.52	0.0113	0.0108	0.407	19.64	17.88	1.85	0.481	0.099
S32750	0.065	1.6	0.0171	0.0049	0.363	23.46	5.16	2.93	0.065	0.133

Table 2: Mechanical properties of alloys S30400, S31254, and S32750.

UNS	Ultimate Strength (Mpa)	Hardness (HV)
S30400	766	303
S31254	969	317
S32750	1146	405

### 2-1: Apparatus of Wear Test:

In this work, a sample grinding machine was used as a wear test machine after adding a cylindrical furnace, temperature-controlled, and a load cell to measure normal load. A 1000W circular heater was installed inside the furnace, as well as a vertical rotating shaft to carry the disc. To measure the inside temperature of the furnace and near the pin, a K-type thermocouple was installed in the center of the cover. Figure 1 illustrates the wear test machine and schematic diagram of details of the furnace.

### 2-2: Wear Test:

Austenitic stainless steel AISI 304 and super austenitic stainless steel S31254 were used as pins and duplex stainless steel AISI 2507 was used as discs. According to the ASTM G 99, (ASTM International, 2012; Sampath, 2015), (Method, 2011), pins of  $\text{Ø}10 \times 70$  mm length and discs of  $\text{Ø}120 \times 4$  mm thickness with an average contact diameter of 85 mm were prepared. The pins were polished and the surface of the discs had an accurate surface finish of  $0.7\mu\text{m}$  on average.

Initially, the pin and disc were cleaned with acetone to prevent the presence of particles between the sliding surfaces and to ensure contact between the metals during the wear test.

To focus on the effect of temperature, in this work, the process parameters of applied load, sliding speed, and sliding distance were set at 45 N, 1.34 m/s, and 2000 m, respectively, because these parameters had already been studied extensively. Five temperature levels were used, from room temperature to  $570^\circ\text{C}$ , as shown in Table 3. The amount of material removal was calculated from the difference in mass of the pins before and after the tests, using Precisa XB 220 A balance with an accuracy of 0.0001 g. Volumetric wear was calculated by subtracting the mass of the pin before and after testing and dividing it by the density of the stainless steel, (Parthasarathi and Duraiselvam, 2010).

Specific wear rate (SWR) is more accurate than volumetric wear in investigating the wear behavior of the materials according to previous works such as (Davanageri, Narendranath and Kadoli, 2018), (Abreu *et al.*, 2015), (Davanageri, Narendranath

and Kadoli, 2019). Therefore SWR is calculated by dividing the volume of wear by the applied load and sliding distance according to the following equation, (Ahmed and Mulapeer, 2021), (Marques *et al.*, 2011).

$$SWR = \frac{W}{D \cdot L} \quad (1)$$

Where W is the volume of removal material in  $\text{mm}^3$ , D is the sliding distance which is constant at 2000 m in this work, and L is the applied load in N.

Table 3: Experimental matrix with volume wear results of AISI 304 and S31254

No.	Temp (°C)	Load (N)	Speed (rpm)	S30400 Wear ( $\text{mm}^3$ )	S31254 Wear ( $\text{mm}^3$ )
1.	30	45	1.34	28.4056	12.1429
2.	140	45	1.34	43.9536	22.7189
3.	300	45	1.34	37.2194	11.5434
4.	460	45	1.34	20.0755	4.8093
5.	570	45	1.34	2.5765	2.1939

### 3. Results

#### 3-1. Effect of Temperature on the Wear Rate

In this work, the influence of ambient temperature on the wear rate of S30400 and S31254 pins with counter surfaces of the S32750 disc was studied. Specific wear rate was calculated using Equation (1) and increased rapidly with increasing temperature from room temperature and the maximum wear rate of S30400 and S31254 occurred at 140°C. After that at 300°C, the wear rate of both alloys initiated to decrease continuously with the increase in temperature, and the minimum wear rate for both alloys was at a temperature of 570°. Furthermore, S31254 exhibited higher wear resistance than the S30400 in all temperatures except at 570°C, where the specific wear rate for both alloys was minimal and nearly equal, as shown in Figure 2.

#### 3-2. Worn Surface Analysis:

SEM images with a magnification of 3.00 and 20.0 KX and the XRD technique of the worn surfaces of both S30400 and S31254 were used to analyze the morphology and composition of the worn surfaces tested at different temperatures. At room temperature, the worn surfaces of both alloys were scratched and direct grooves were formed, but the grooves in S30400 were deeper and exfoliating,

and plastic deformations were formed, as shown in Figures 3-A and B. The XRD peaks of both alloys are similar and there are no oxide phases, as shown in Figures 3-C and D. Sever worn surfaces with deep grooves, cracks, and plastic deformation can be seen on both surfaces in Figures. 4-A and B that tested at 140°C. As in the room temperature tests, the XRD peaks consist of the composition of the alloys without any formation of oxides, and the peaks in Figures 4-C and D of S30400 and S31254 are very similar because both are in the same stainless steel family but with different amounts of elements. At 300°C, the formation of oxides began to the formation on the worn surfaces. In the SEM images in Figure 5-A, grooves and plastic deformation can be seen, while in S31254 only direct grooves appear, as in Figure 5-B. XRD analysis showed the formation of chromite and hematite in S30400, while magnetite arose on the surface of S31254, as shown in Figures 5-C and D. In addition to the formation of oxide layers, as shown by the XRD analysis of both alloys in Figures 6-C and D, deep grooves, cracks, holes, and plastic deformation appeared on the surface of S30400 at 460°C, while lighter grooves appeared on the oxidizing surfaces of S31254, as shown in Figures 6-A and B. At 570°C, the surfaces of S30400 and S31254 were completely covered with oxides such as chromite, hematite, and iron oxides, as confirmed by the XRD results, as shown in the Figures 7-C and D. Moreover, plastic deformation, exfoliating, cracks, and holes appeared on the

surface of S30400, while deep grooves and minor plastic deformation were observed on the surface of S31254, as shown in Figures 7-A and B.

#### 4. Discussion:

The significant difference in specific wear rate between S30400 and S31254 in Figure 2 shows that the specific wear rate of S30400 was twice or higher than that of S31254 in all cases except at 570°C. The high wear resistance of S31254 compared to S30400 is attributed to its high strength and hardness, as shown in Table 2. According to Archard's law, wear is inversely proportional to the hardness of the worn surface or the weaker surface between a pair of sliding surfaces. However, the difference in hardness between S30400 and S31254 was relatively small, the strength of S31254 was 969 MPa, and 22% higher than that of S30400, which reduces plastic deformation and cracking. In addition, S31254 contains more chromium and molybdenum, as shown in Table 1, which improves the corrosion, pitting, and wear resistance.

The wear rate increased with the increase of temperature from room temperature to 140°C since an increase in temperature leads to a decrease in hardness and strength. Furthermore, wider grooves, cracks, and plastic deformation were observed in the samples tested at 140°C compared to those tested at room temperature. On the other hand, the XRD pattern for both alloys at room temperature

and 140°C was completely the same, which emphasizes that no oxides occur on the surfaces, as shown in Figures 3 and 4.

On the other hand, the wear rate decreased from 300°C to 570°C due to the formation of oxides on the worn surfaces since oxide phases have high hardness and act as self-lubricants reducing friction. At 300°C, the SEM images of both alloys with a magnification of 20 KX exhibited that the surfaces were partially covered by oxides, as shown in Figures 8-A and B, therefore wear rate decreased compared with lower temperatures. At 460°C, the wear rate significantly decreased due to larger areas of the surfaces were covered with oxide layers, and traces of wear as well as remaining deposits were observed, as shown in Figures 8-C and D. At 570°C the surfaces of S30400 and S31254 were completely covered with oxides, while small debris adhered to the surface of S31254. Both surfaces were completely covered by almost the same oxides, which made the surfaces hard and well self-lubricating so that the wear rates were at a minimum and partially the same, as shown in Figures 8-E and F. In all experiments, the surface of S30400 was more worn compared to the surface of S31254, as well as material removal and wear rate was higher. Consequently, S31254 is a reasonable and preferable substitute for S30400 in important applications and especially at high temperatures.

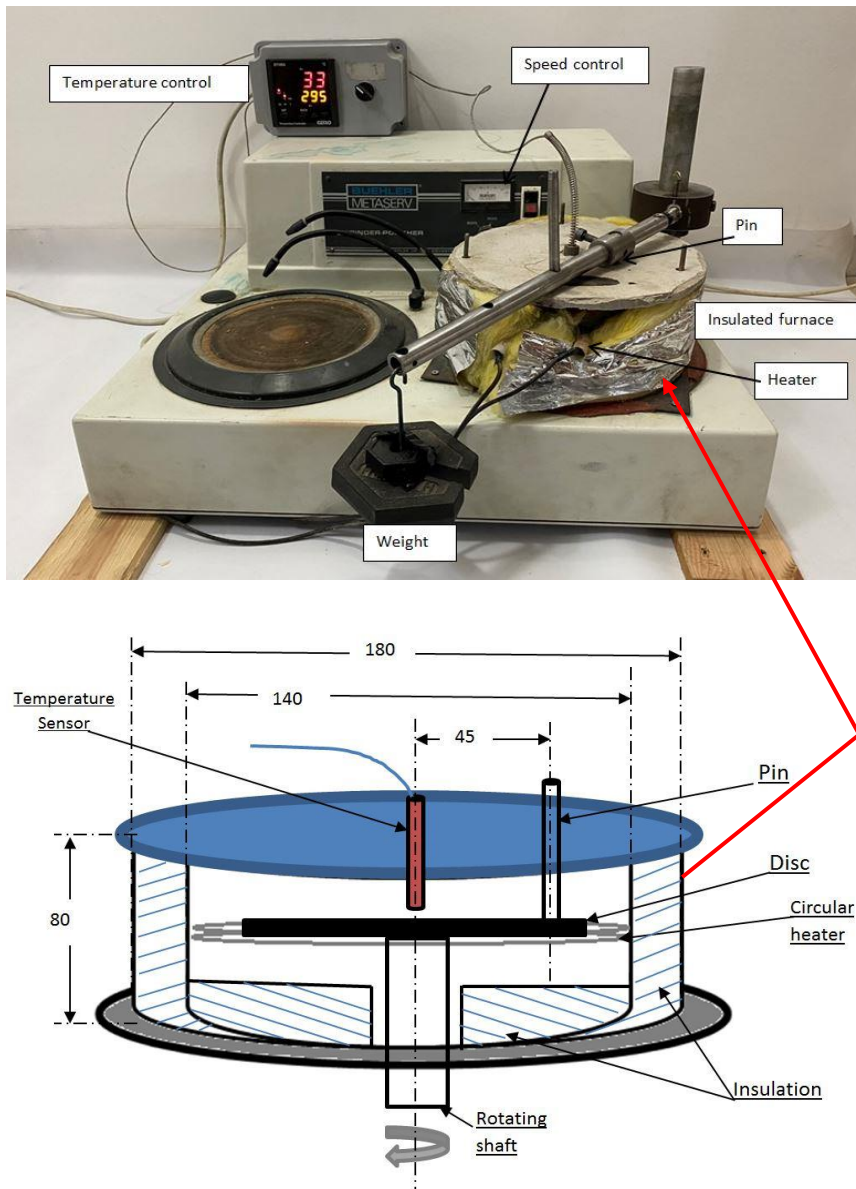


**Figure 1:** a) Wear machine with the furnace, temperature control, carriage of weight, and pin holder. b) Schematic diagram of the furnace with necessity dimensions.

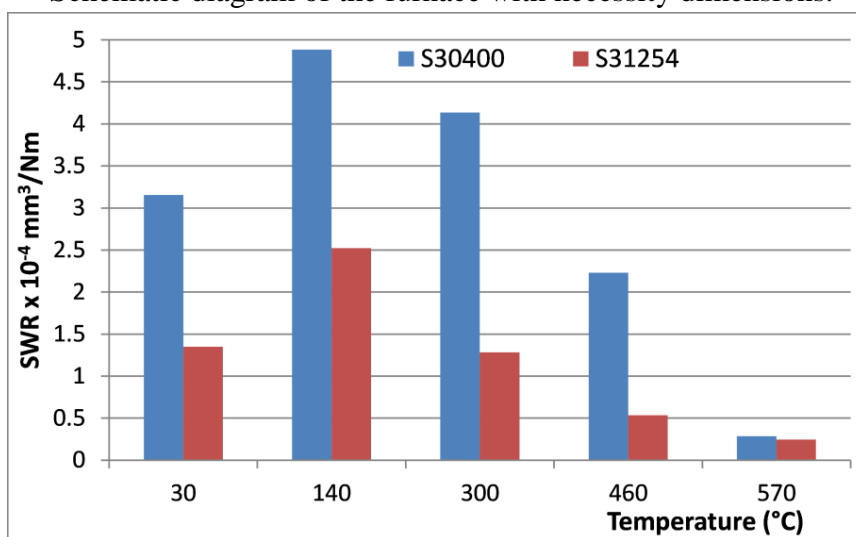


**Figure 2.** Effect of temperature on the specific wear rate of S30400 and S31254 austenitic and super austenitic stainless steel at 45N, 1.34 m/s, and 2000 m

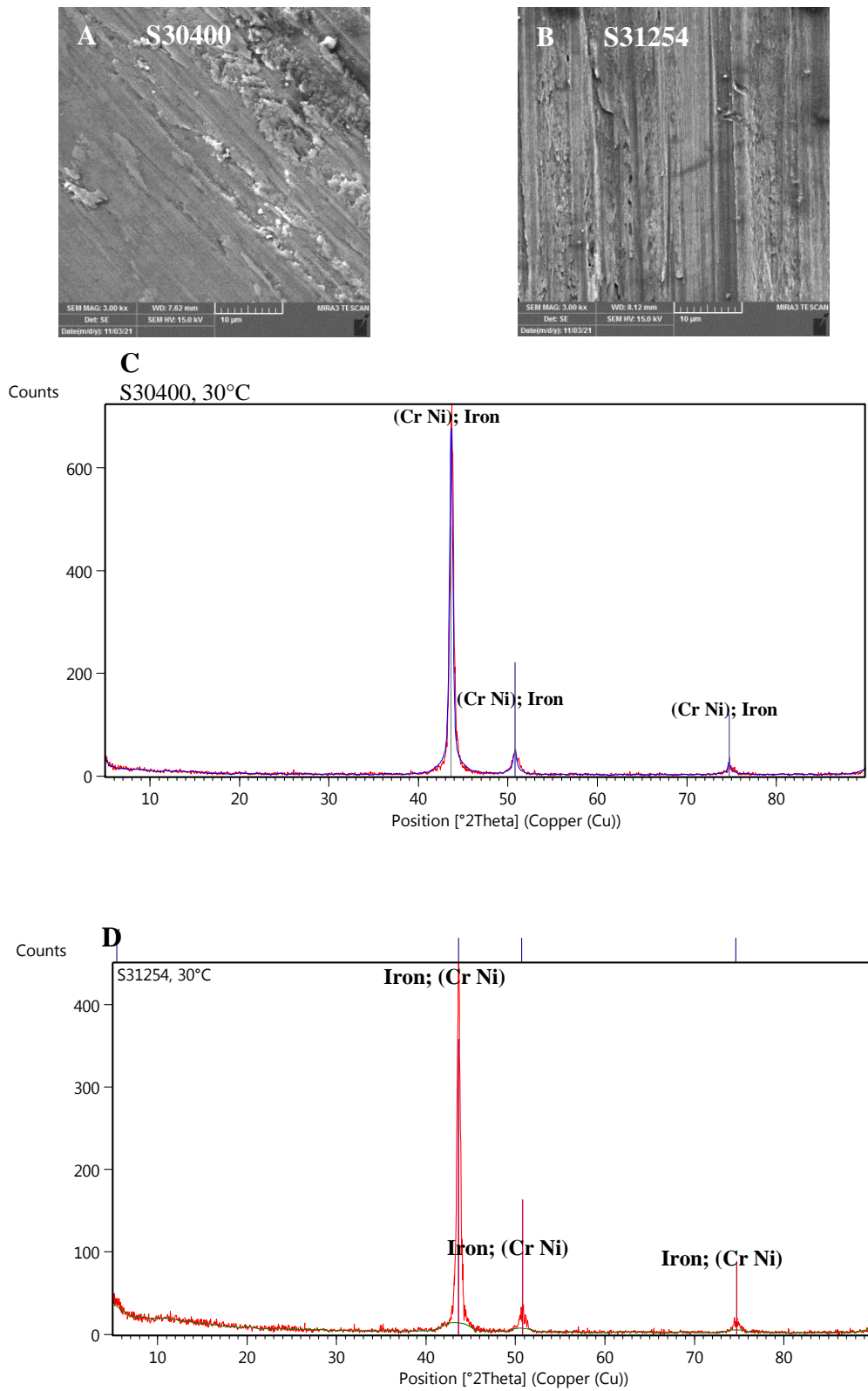


**Figure 3.** SEM image with a magnification of 3 KX and XRD technique of worn surface of S30400 and S31254 at 1.34 m/s, 45 N, 2000 m, and 30°C

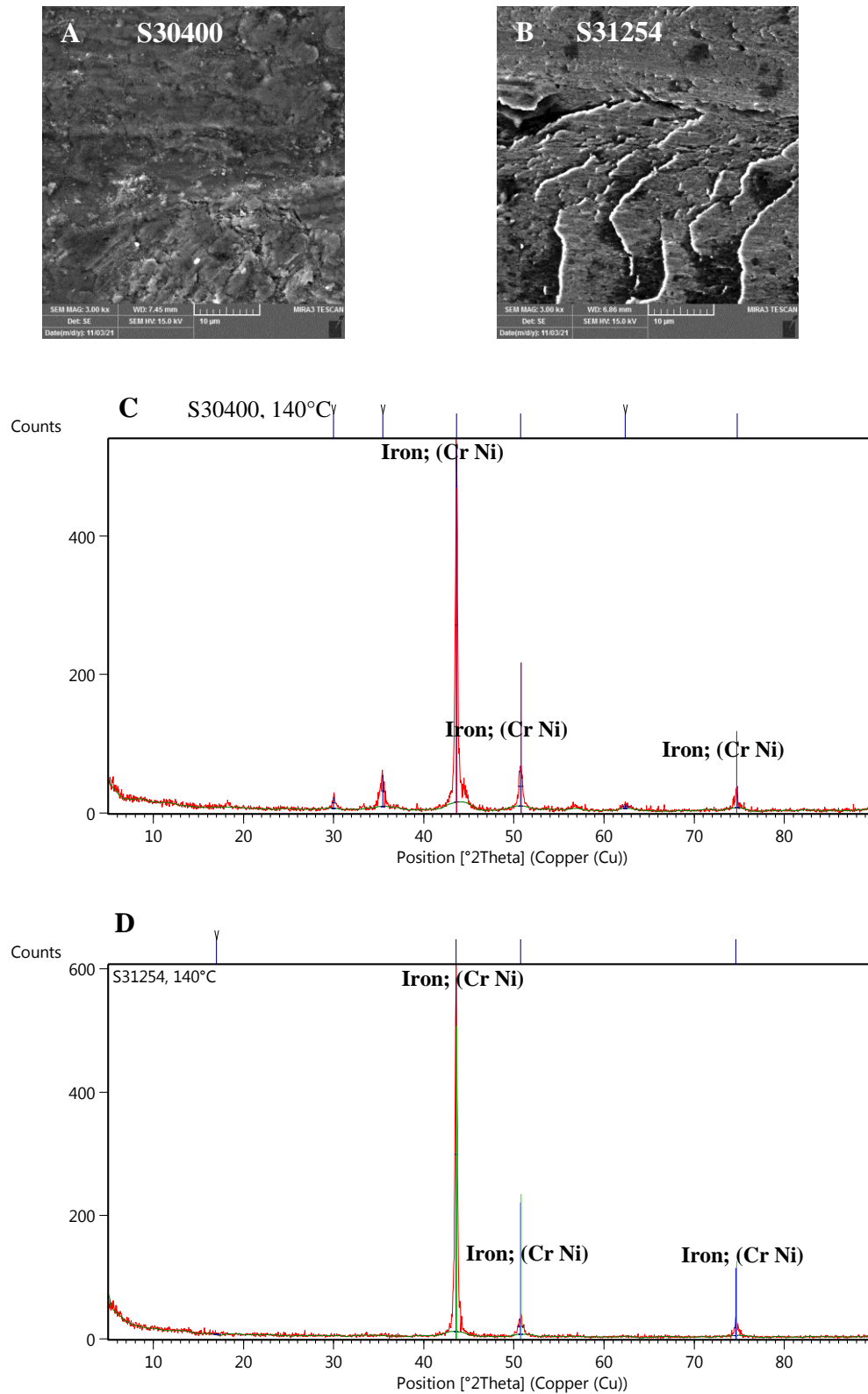


**Figure 4.** SEM image with 3 KX and XRD technique of worn surface of S30400 and S31254 at 1.34 m/s, 45 N, 2000 m, and 140°C

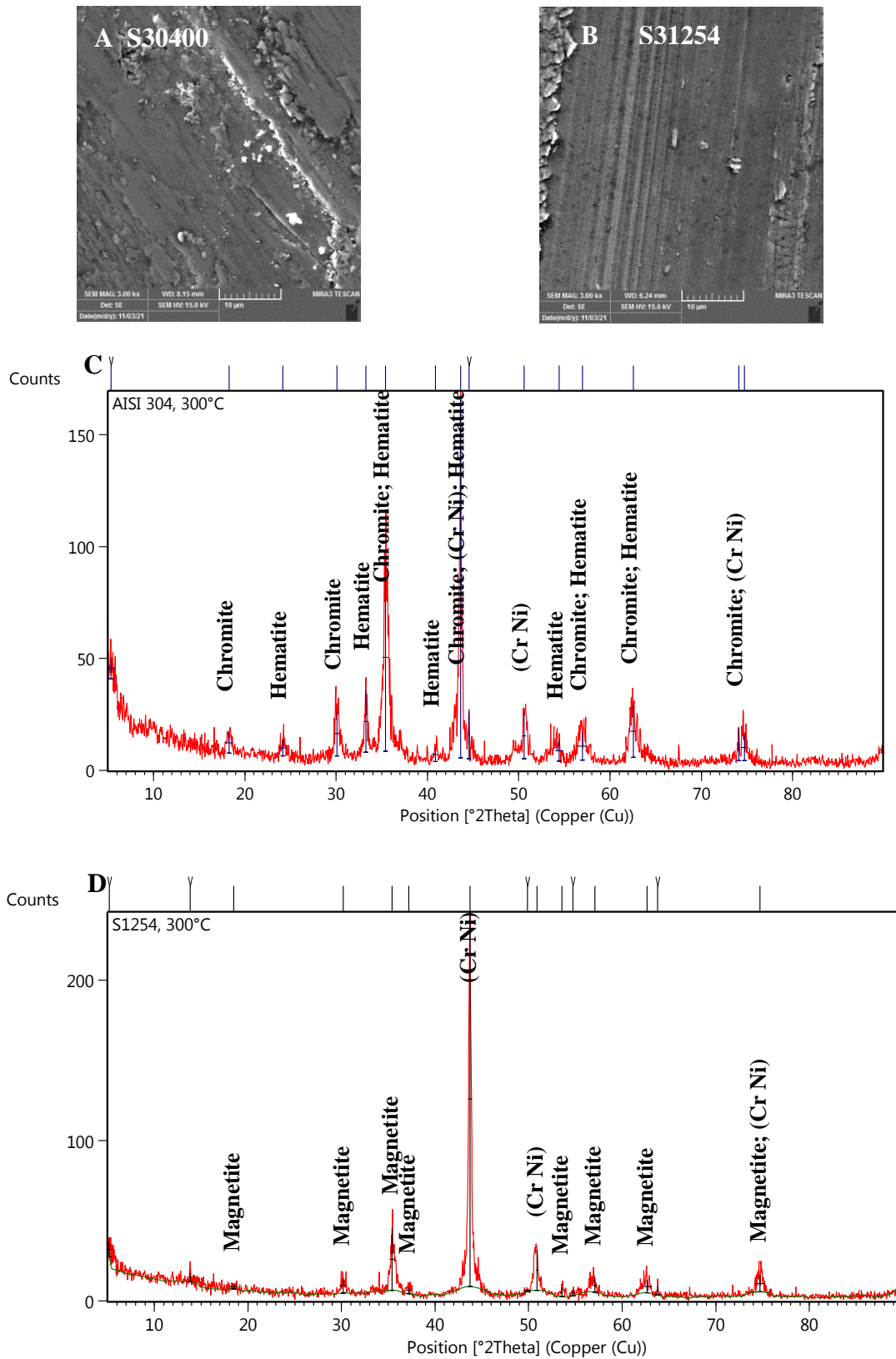


**Figure 5.** SEM image with 3 KX and XRD technique of worn surface of S30400 and S31254 at 1.34 m/s, 45 N, 2000 m, and 300°C

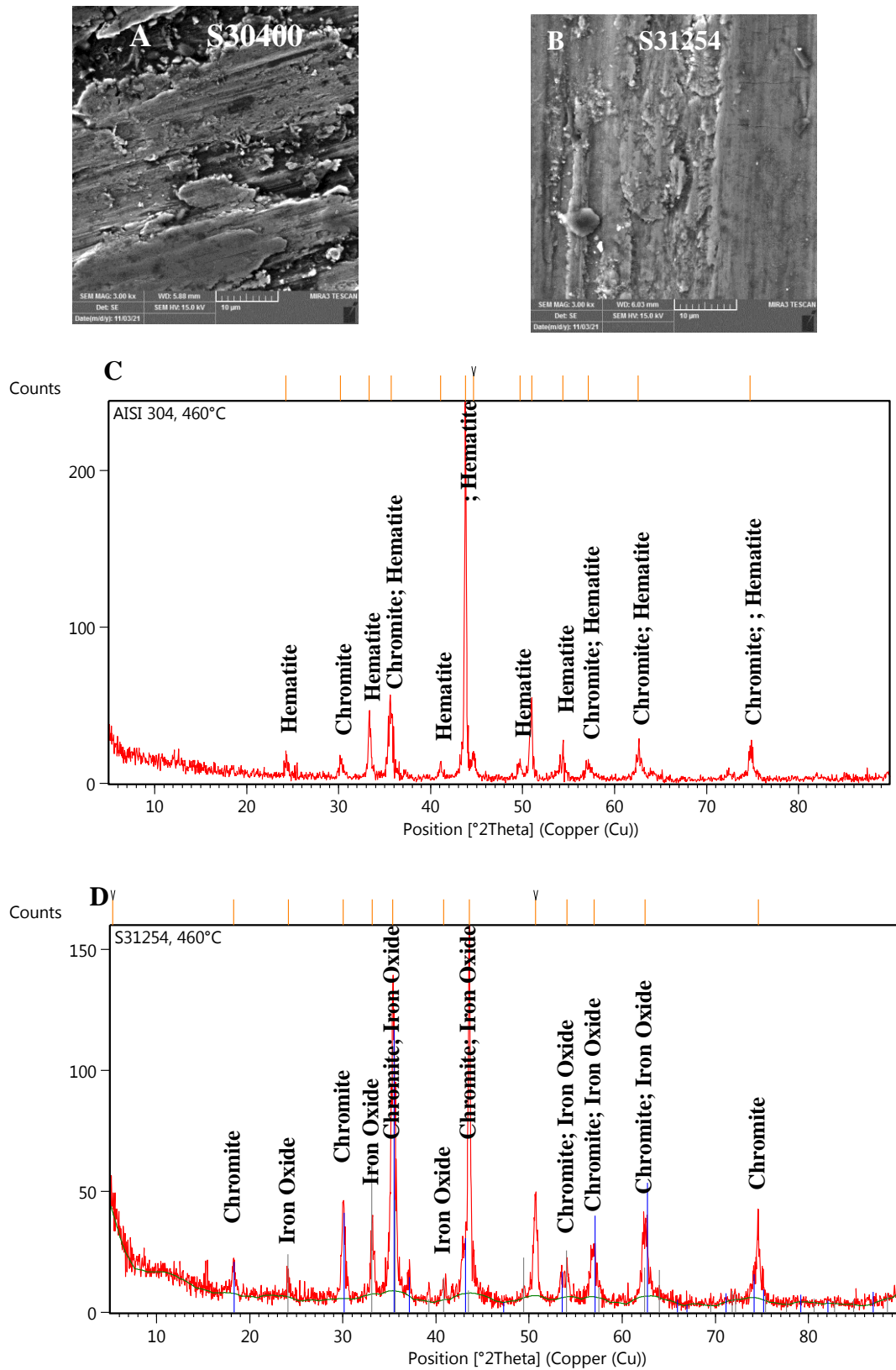


**Figure 6.** SEM image with 3 KX and XRD technique of worn surface of S30400 and S31254 at 1.34 m/s, 45 N, 2000 m, and 460°C

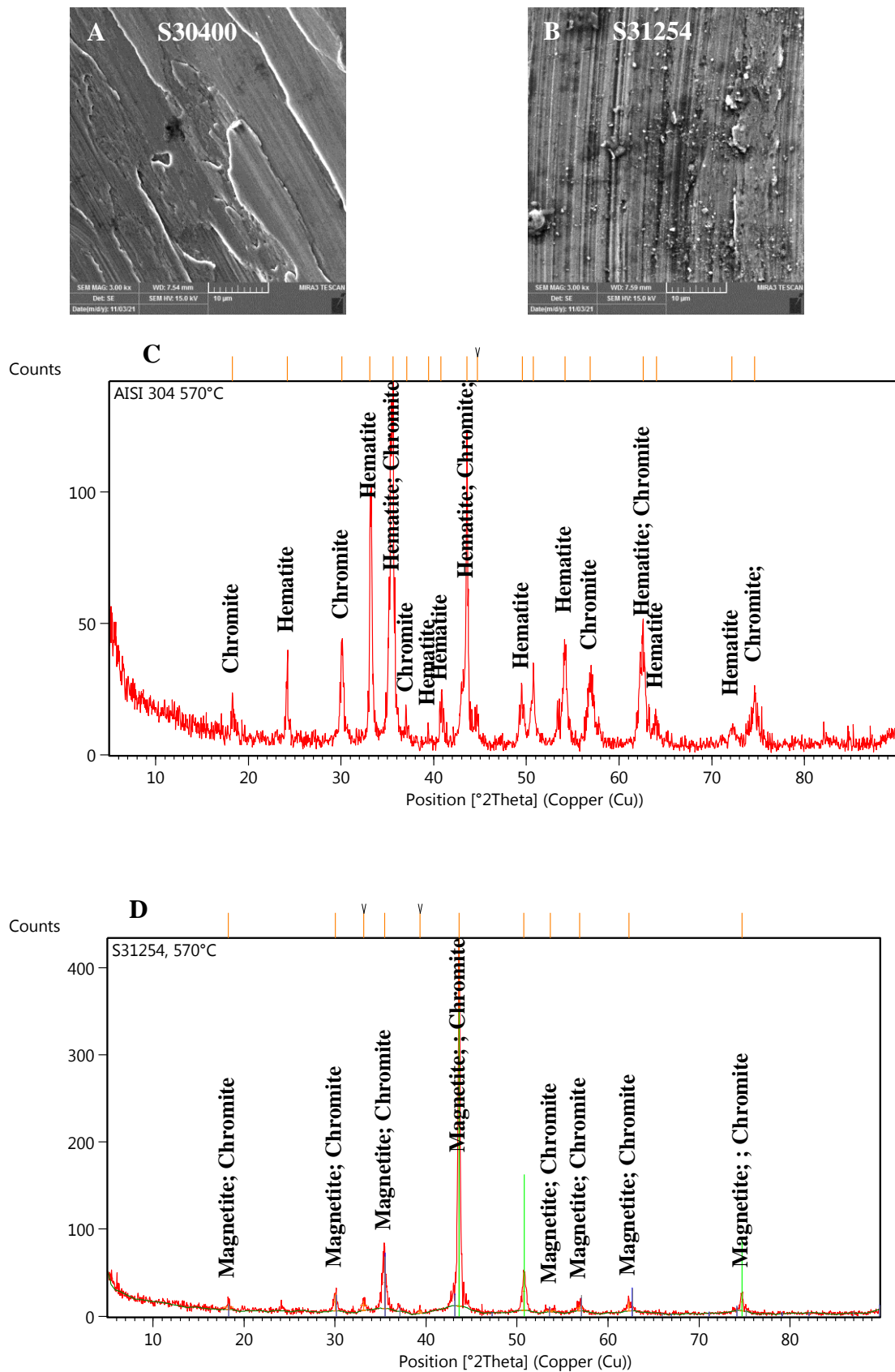


**Figure 7.** SEM image and XRD technique of worn surface of S30400 and S31254 at 1.34 m/s, 45 N, 2000 m, and 570°C

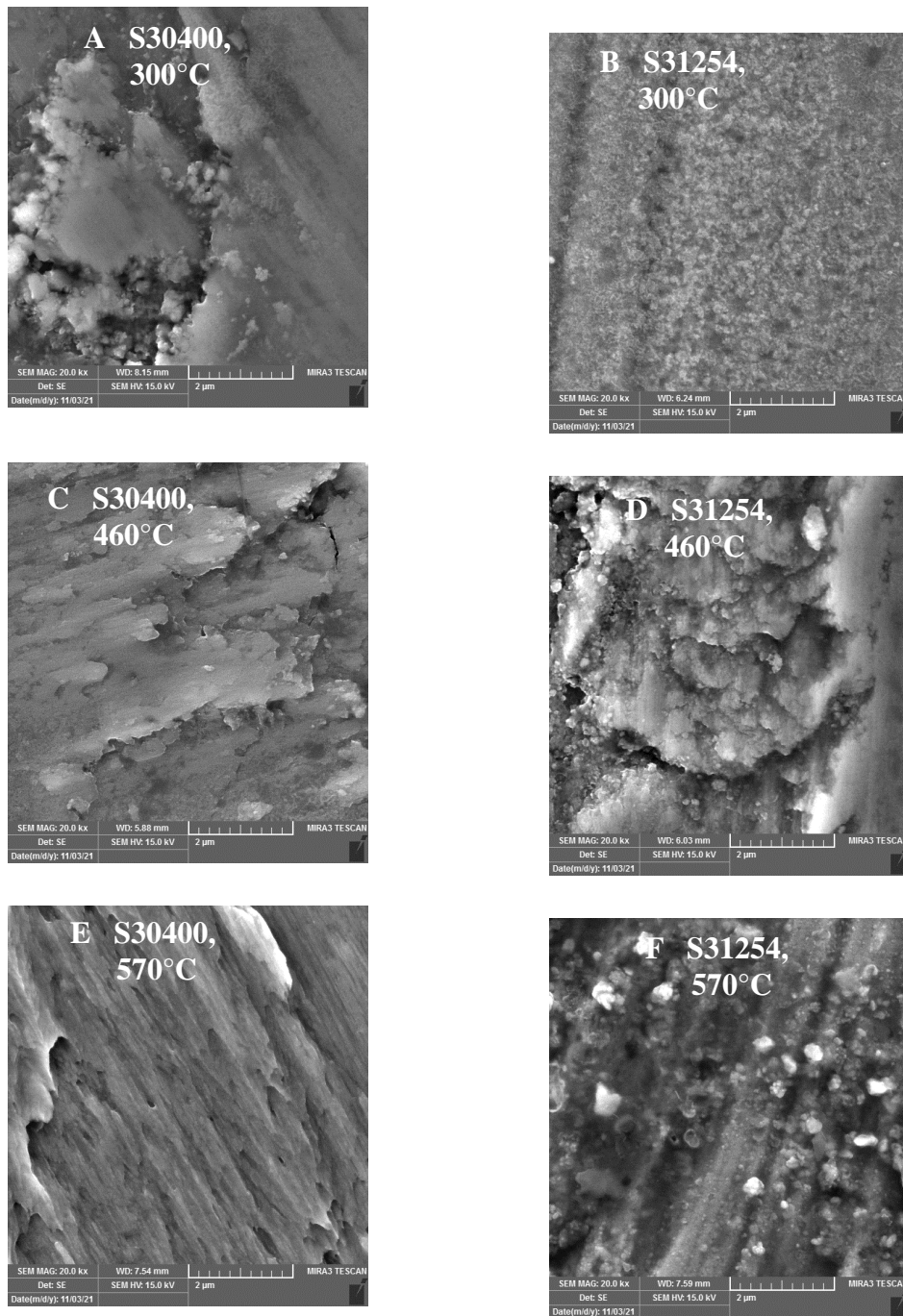


**Figure 8.** SEM image of worn surfaces of S30400 and S31254 at 300°C, 460°C, and 570°C with a magnification of 20.0 KX

## 5. Conclusion

In this study, the effect of temperature on the specific wear rate of S30400 and S31254 versus super duplex stainless steel was investigated. The morphology and formation of the worn surfaces were studied using SEM and XRD techniques. As a result of this work, the following observations and findings were obtained:

1. From room temperature to 460°C, the specific wear rate of S30400 is significantly higher than

that of S31254. At 570°C and due to the complete formation of oxide layers, the specific wear rate is partially similar for both alloys.

2. The specific wear rate for both alloys increases with the increase of temperature from room temperature to 140°C and then decreases significantly due to the formation of oxide phases such as chromite, hematite, and magnetite in both alloys.

3. The images from SEM deduced that the surface of S30400 is highly worn compared to S31254 under the same wear conditions in terms of deeper grooves, more plastic deformation, and exfoliating.
4. The morphology of the worn surfaces, studied using SEM images and XRD analyses, showed that the oxide phases begin to form at 300°C and increase with increasing temperature. The oxide layers act as a protective glaze layer on the worn surfaces of both alloys.
5. For special and high-temperature applications, S31254 is recommended instead of the austenitic stainless steel S30400.

#### Conflict of Interest:

The authors declare no conflict of interest.

#### References:

- Abreu, C. M. *et al.* (2015) 'Wear and corrosion performance of two different tempers (T6 and T73) of AA7075 aluminium alloy after nitrogen implantation', *Applied Surface Science*. Elsevier B.V., 327, pp. 51–61. doi: 10.1016/j.apsusc.2014.11.111.
- Ahmed, D. A. and Mulapeer, M. M. (2021) 'Modeling Wear Rate of Super Austenitic Stainless Steel S31254 at Elevated Temperature by Response Surface Methodology', *Design Engineering (TORONTO)*, (8), pp. 4334–4348.
- Alabdullah, M. *et al.* (2017) 'Effect of Microstructure on Chip Formation during Machining of Super Austenitic Stainless Steel', *International Journal of Materials Forming and Machining Processes*, 4(1), pp. 1–18. doi: 10.4018/ijmfmp.2017010101.
- Alabdullah, M., Polishetty, A. and Littlefair, G. (2016) 'Impacts of Wear and Geometry Response of the Cutting Tool on Machinability of Super Austenitic Stainless Steel', *International Journal of Manufacturing Engineering*, 2016. doi: 10.1155/2016/7213148.
- Alvi, S., Saeidi, K. and Akhtar, F. (2020) 'High temperature tribology and wear of selective laser melted (SLM) 316L stainless steel', *Wear*. Elsevier B.V., 448–449(January), p. 203228. doi: 10.1016/j.wear.2020.203228.
- ASTM E8 (2010) 'ASTM E8/E8M standard test methods for tension testing of metallic materials 1', *Annual Book of ASTM Standards 4*, (C), pp. 1–27. doi: 10.1520/E0008.
- ASTM International (2012) 'E407-07: Standard Practice for Microetching Metals and Alloys', *ASTM International*, West Conshohocken, PA, pp. 1–21.
- ASTM Standard E92-82 (1997) 'ASTM E92-82 Standard Test Method for Vickers Hardness of Metallic Materials', *Annual Book of ASTM Standards 4*, 82(Reapproved), pp. 1–27.
- Avilaa, B. M. R. *et al.* (2020) 'Cold Deformation and Hardness on Superaustenitic Stainless Steel: Evaluation Methods', *Materials Research*, 23(4). doi: 10.1590/1980-5373-MR-2020-0210.
- Bahshwan, M. *et al.* (2020) 'The role of microstructure on wear mechanisms and anisotropy of additively manufactured 316L stainless steel in dry sliding', *Materials and Design*. The Authors, 196, p. 109076. doi: 10.1016/j.matdes.2020.109076.
- Bayata, F. and Alpas, A. T. (2021) 'The high temperature wear mechanisms of iron-nickel steel (NCF 3015) and nickel based superalloy (inconel 751) engine valves', *Wear*. Elsevier B.V., 480–481(September 2020), p. 203943. doi: 10.1016/j.wear.2021.203943.
- Chawla, K. *et al.* (2013) 'Investigation of tribological behavior of stainless steel 304 and grey cast iron rotating against EN32 steel using pin on disc apparatus', *IOSR Journal of Mechanical*, 9(4), pp. 18–22.
- Davanageri, M. B., Narendranath, S. and Kadoli, R. (2018) 'Finite Element Wear Behaviour Modeling of Super duplex stainless steel AISI 2507 Using Ansys', *IOP Conference Series: Materials Science and Engineering*, 376(1). doi: 10.1088/1757-899X/376/1/012131.
- Davanageri, M. B., Narendranath, S. and Kadoli, R. (2019) 'Modeling and Optimization of Wear Rate of AISI 2507 Super Duplex Stainless Steel', *Silicon*, 11(2), pp. 1023–1034.
- Ge, S. *et al.* (2019) 'Preparation and characterization of a new type of 304 stainless steel metallocking key', *IOP Conference Series: Earth and Environmental Science*, 358(5). doi: 10.1088/1755-1315/358/5/052062.
- Hernandez, S. *et al.* (2014) 'High temperature friction and wear mechanism map for tool steel and boron steel tribopair', *Tribology - Materials, Surfaces and Interfaces*, 8(2), pp. 74–84. doi: 10.1179/1751584X13Y.0000000049.
- Kennedy, F. E., Lu, Y. and Baker, I. (2015) 'Contact temperatures and their influence on wear during pin-on-disk tribotesting', *Tribology International*. Elsevier, 82(PB), pp. 534–542. doi: 10.1016/j.triboint.2013.10.022.
- Li, L. *et al.* (2019) 'Enhanced Wear Resistance of Iron-Based Alloy Coating Induced by Ultrasonic Impact', *coatings*, 804(9), pp. 1–14.
- Marques, F. *et al.* (2011) 'Influence of heat treatments on the micro-abrasion wear resistance of a superduplex stainless steel', *Wear*. Elsevier B.V., 271(9–10), pp. 1288–1294. doi: 10.1016/j.wear.2010.12.087.
- Method, S. T. (2011) 'Standard Test Method for Wear Testing with a Pin-on-Disk Apparatus 1', *Wear*, 05(Reapproved 2010), pp. 1–5. doi: 10.1520/G0099-05R10.2.
- Moharana, B. R. *et al.* (2016) 'Experimental investigation on mechanical and microstructural properties of AISI 304 to Cu joints by CO2 laser', *Engineering Science and Technology, an International Journal*. Elsevier B.V., 19(2), pp. 684–690. doi:

- 10.1016/j.jestch.2015.10.004.
- Monga, A., Gumber, S. and Grover, H. (2018) 'Study of Abrasion Wear and Factors Affecting Wear Rate', *Advance Research in Science and engineering*, 7(23198354), pp. 113–120.
- Parthasarathi, N. L. . and Duraiselvam, M. (2010) 'Improvement of High Temperature Wear Resistance of AISI 316 ASS through NiCrBSiCFe Plasma Spray Coating', *Journal of Minerals and Materials Characterization and Engineering*, 09(07), pp. 653–670. doi: 10.4236/jmmce.2010.97047.
- Parthasarathi, N. L., Borah, U. and Albert, S. K. (2013) 'Correlation between coefficient of friction and surface roughness in dry sliding wear of AISI 316 L (N) stainless steel at elevated temperatures', *Computer Modelling and New Technologies*, 17(1), pp. 51–63.
- Polishetty, A., Alabdullah, M. and Littlefair, G. (2017) 'Tool Wear Analysis due to Machining in Super Austenitic Stainless Steel', *MATEC Web of Conferences*, 95, pp. 4–7. doi: 10.1051/mateconf/20179505006.
- Qiao, Y. *et al.* (2019) 'Effect of solution treatment on cavitation erosion behavior of high-nitrogen austenitic stainless steel', *Wear*. Elsevier B.V., 424–425(January), pp. 70–77. doi: 10.1016/j.wear.2019.01.098.
- Rababa, K. S. and Al-Mahasne, M. M. (2011) 'Effect of roller burnishing on the mechanical behavior and surface quality of O1 alloy steel', *Research Journal of Applied Sciences, Engineering and Technology*, 3(3), pp. 227–233.
- Sampath, P. S. (2015) 'Wear and Corrosion Studies on Ferritic Stainless Steel (Ss 409M)', *International Journal of Research in Engineering and Technology*, 04(04), pp. 502–511. doi: 10.15623/ijret.2015.0404088.
- Sathiya, P., Mishra, M. K. and Shanmugarajan, B. (2012) 'Effect of shielding gases on microstructure and mechanical properties of super austenitic stainless steel by hybrid welding', *Materials and Design*. Elsevier Ltd, 33(1), pp. 203–212. doi: 10.1016/j.matdes.2011.06.065.
- Singh, J., Sharma, S. and Singh, A. P. (2019) 'Oxidation Effects on wear Resistance of SS-304 and SS-316 Austenitic Stainless Steels', *International Journal of Innovative Technology and Exploring Engineering (IJITEE)*, 8(10), pp. 2353–2357.
- Suthar, F. *et al.* (2015) 'Comparative Evaluation of Abrasive Wear Resistance of Various Stainless Steel Grades', *Ge-International Journal of Engineering Research*, 3(7), pp. 20–35.
- Zhang, Y., Yin, X. Y. and Yan, F. Y. (2016) 'Tribocorrosion behaviour of type S31254 steel in seawater: Identification of corrosion-wear components and effect of potential', *Materials Chemistry and Physics*. Elsevier B.V, 179, pp. 273–281. doi: 10.1016/j.matchemphys.2016.05.039.